https://communications.science.ankara.edu.tr

Commun.Fac.Sci.Univ.Ank.Ser. A1 Math. Stat.
Volume 70, Number 2, Pages 871–887 (2021)
DOI: 10.31801/cfsuasmas.906339
ISSN 1303–5991 E-ISSN 2618–6470

Research Article; Received: March 30, 2021; Accepted: May 4, 2021

INVERSE STEREOGRAPHIC HYPERBOLIC SECANT DISTRIBUTION: A NEW SYMMETRIC CIRCULAR MODEL BY ROTATED BILINEAR TRANSFORMATIONS

Abdullah YILMAZ

Department of Actuarial Sciences, Kirikkale University, TURKEY

Abstract. The inverse stereographic projection (ISP), or equivalently, bilinear transformation, is a method to produce a circular distribution based on an existing linear model. By the genesis of the ISP method, many important circular models have been provided by many researchers. In this study, we propose a new symmetric unimodal/bimodal circular distribution by the rotated ISP method considering the hyperbolic secant distribution as a baseline distribution. Rotation means that fixing the origin and rotating all other points the same amount counterclockwise. Considering the effect of rotation on the circular distribution to be obtained with the bilinear transformation, it is seen that it actually induces a location parameter in the obtained circular probability distribution. We analyze some of the stochastic properties of the proposed distribution. The methods for the parameter estimation of the new circular model and the simulation-based compare results of these estimators are extensively provided by the paper. Furthermore, we compare the fitting performance of the new model according to its well-known symmetric alternatives, such as Von-Misses, and wrapped Cauchy distributions, on a real data set. From the information obtained by the analysis on the real data, we say that the fitting performance of the new distribution is better than its alternatives according to the criteria frequently used in the literature.

1. INTRODUCTION

Circular or directional data are observed in various fields of science. Data on angular observations can often be associated with compass measurements. Additionally, daily, weekly, or hourly observations obtained in the specific time period

2020 *Mathematics Subject Classification.* 62H11, 60E05, 62F10, 62E15.
Keywords. Circular distribution, inverse stereographic, bilinear transformation, Möbius transformation, rotation.

a.yilmaz@kku.edu.tr
0000-0002-1196-9541.

may be circular. Although it may seem attractive in some ways, processing and evaluating such data linearly can lead to false results. In directional data, the start and endpoints are neighbors despite having the furthest distance according to linear metric. As a simple example, the arithmetic mean of two angles 1 and 359 degrees is 180 degrees, although the circular average to be 0 degrees. Therefore, it requires a special class of distributions known as circular probability distributions to analyze such data.

Circular probability distributions are usually obtained by circularizing a known linear probability distribution. The two most common methods for circularization are wrapping and inverse stereographic projection (ISP). ISP method is based on bilinear transformations. Minh and Farnum [8] used bilinear transformations to map points on the unit circle in the complex plane into points on the real line. Thus, they used the stereographic projection as a transformation, to produces probability distributions on the real line by circular models. It was clear that by the inverse of this transformation (ISP), circular probability distributions could be obtained from probability distributions on the real line. Many studies on circular distributions obtained using the ISP method have been added to the literature. Yedlapalli, et al [11] used to transformation on double Weibull distribution to obtain a symmetric circular distribution. Kato and Jones [6] proposed a family of four-parameter distributions on the circle that contains the Von Mises and wrapped Cauchy distributions as special cases. Girija, et al [5] introduced stereographic double exponential distribution obtained by using double exponential (Laplace) distribution. The same authors introduced the stereographic logistic model [2] in a later study. Yedlapalli, et al [12] obtained semicircular (axial) model induced by using modified inverse stereographic projection on Quasi Lindley distribution. The projection method used in all these studies is based on the result obtained by Minh and Farnum [8] in a study in which they introduced the induction of linear models with Möbius transformations. Möbius transformation (bilinear, fractional linear or linear fractional transformation) provides very convenient methods of finding a one-to-one mapping of one domain into another. In a general form, Möbius transformation can be written as

$$\mathrm{T}\left(z\right)=\frac{az+b}{cz+d}, \tag{1}$$

where a,b,c and d are complex or real valued coefficients and $bc-ad\neq 0$. This transformation was proposed by Minh and Farnum [8] as a new method of generating probability distributions, which maps every point on a real line onto the point on a unit circle. Their construction proceeds as follows. In order for $T\left(z\right)$ to map the unit circle on the real line, the constraints $\mathrm{Im}\left(c\right)\neq 0$, $\overline{a}d=\overline{c}b$, and $a\neq 0$ must be provided. Dividing all coefficients in Eq.(1) by a and imposing the requirement $T\left(-1\right)=\infty$ yields the transformation of the form

$$\mathrm{T}\left(z\right)=\frac{cz+\overline{c}}{z+1}. \tag{2}$$

Finally, by taking $c = u - iv$ and $z = \cos(\theta) + i\sin(\theta)$, the transformation

$$x = T(\theta) = \mathrm{T}(\cos(\theta) + i\sin(\theta))$$
$$= u + v\frac{\sin(\theta)}{1+\cos(\theta)} = u + v\tan\left(\frac{\theta}{2}\right) \tag{3}$$

is obtained which is known as stereographic transformation. Inverse stereographic projection yields a circular model when it applied to a linear model. If a random variable is defined on the whole real line with probability density function (pdf) $f(.)$ and cumulative distribution function (cdf) $F(.)$ then $\Theta = T^{-1}(X)$ is a random point on the unit circle, with the pdf $g(.)$ and the cdf $G(.)$, respectively, defined as

$$g(\theta) = f(T(\theta))\left|\frac{d}{d\theta}T(\theta)\right| = f\left(u + v\tan\left(\frac{\theta}{2}\right)\right)\frac{v}{\cos(\theta)+1}, \tag{4}$$

$$G(\theta) = F(T(\theta)) = F\left(u + v\tan\left(\frac{\theta}{2}\right)\right), \tag{5}$$

where $\theta \in [-\pi, \pi)$, $u \in \mathbb{R}$ and $v > 0$. Multiplying the coefficients in Eq.(1) by k yields one to one and the same mapping, where k is an arbitrary (non-zero) complex number. Since three complex numbers are sufficient to pin down the mapping, i.e., there exist a unique Mobius transformation sending any three points (z_1, z_2, z_3) to any other three points (w_1, w_2, w_3) [9]. Consider the cross-ratio of three points

$$(z, z_1, z_2, z_3) = \frac{(z - z_1)(z_2 - z_3)}{(z - z_3)(z_2 - z_1)}.$$

where $z_i \neq z_j, i, j = 1, 2, 3$ and $i \neq j$. Then there is a unique Mobius transformation such that

$$(z, z_1, z_2, z_3) = (w, w_1, w_2, w_3).$$

Moreover, it is known that rotation is to fix the origin and spin all other points counter-clockwise by the same amount (see Fig.1). By this motivation, if we solve the equation

$$\left(z, e^{-i\alpha}, e^{-i(\alpha-\pi/2)}, e^{-i(\alpha+\pi/2)}\right) = (w, u, u+v, u-v)$$

with respect to w, we have

$$w = \mathrm{T}_\alpha(z) = u - iv\left(1 - \frac{2}{1+e^{i\alpha}z}\right). \tag{6}$$

Note that, multiplication z by $e^{i\alpha}$ has a geometric effect of anti-clockwise rotation about the origin by an angle of $\alpha \in [-\pi, \pi)$. So, it is easy to see that $\mathrm{T}_\alpha(z) = \mathrm{T}\left(e^{i\alpha}z\right)$. Finally, by taking $z = \cos(\theta) + i\sin(\theta)$ in Eq.(6), we have

$$x = T_\alpha(\theta) = \mathrm{T}_\alpha(\cos(\theta) + i\sin(\theta))$$
$$= u + v\tan\left(\frac{\theta+\alpha}{2}\right). \tag{7}$$

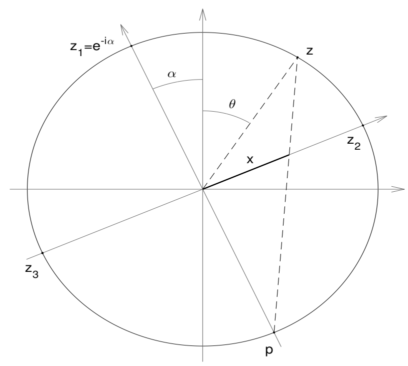

FIGURE 1. Rotation by α, cross-ratio points z_1, z_2, z_3 and pole (p).

Lemma 1. *Pole of transformation in Eq.(6) is* $z = -e^{-i\alpha}$.

Lemma 2. *Inverse transformation of* T_α *is* $T_\alpha^{-1}(x) = 2\tan^{-1}\left(\frac{x-u}{v}\right) - \alpha$.

Lemma 3. *Let* X *be a random variable defined on* $(-\infty, \infty)$ *with pdf* $f(.)$ *and cdf* $F(.)$. *Then* $\Theta = T_\alpha^{-1}(X)$ *is a circular random variable with pdf*

$$g(\theta;\alpha) = f(T_\alpha(\theta)) \left| \frac{d}{d\theta} T_\alpha(\theta) \right|$$
$$= f\left(u + v\tan\left(\frac{\theta+\alpha}{2}\right)\right) \frac{v}{\cos(\theta+\alpha)+1}, \tag{8}$$

and the corresponding cdf

$$G(\theta;\alpha) = F(T_\alpha(\theta)) = F\left(u + v\tan\left(\frac{\theta+\alpha}{2}\right)\right), \tag{9}$$

where $\alpha \in [-\pi, \pi)$, $v > 0$ *and* $u \in \mathbb{R}$.

The probability density function given by the Eq.(8) provides three properties: i) $g(\theta;\alpha) \geq 0$ for $\forall\theta \in \mathbb{R}$, ii) $g(.)$ is periodic with period 2π, iii) $\int_\Gamma g(\theta;\alpha)\,d\theta = 1$ where Γ is any interval of length 2π.

Proposition 4. *A rotation of Mobius transformation given by the Eq.(2) will induce a location parameter in the probability distribution given by the Eq.(4).*

Proof. Proof is clear from lemma 3. □

Corollary 5. *The quantile function of* $\Theta = T_\alpha^{-1}(X)$ *is*

$$Q(t) = 2\tan^{-1}\left(\frac{F^{-}(t) - t}{v}\right) - \alpha, \tag{10}$$

where $t \in (0,1)$, $F^{-}(t) = \inf\{x \in \mathbb{R} : F(x) \geq t\}$ *and* $F(.)$ *is the cdf of random variable* X*.*

Proposition 6. *Let* X *be a symmetric random variable around* $E(X) = u$*. The random variable* Θ *defined as* $\Theta = T_{\alpha}^{-1}(X)$ *has a symmetrical distribution around* $-\alpha$*.*

Proof. If X is symmetric around $E(X) = u$ then, $F^{-}(1/2) = u$ and $F^{-}\left(\frac{1}{2} - r\right) + F^{-}\left(\frac{1}{2} + r\right) = 2u$, where $0 < r < 1/2$ and $F^{-}$is the quantile function of X. Thus $Q\left(\frac{1}{2}\right) = -\alpha$ and

$$\begin{aligned} Q\left(\tfrac{1}{2} - r\right) + Q\left(\tfrac{1}{2} + r\right) &= 2\tan^{-1}\left(\frac{F^{-}\left(\frac{1}{2}-r\right)-u}{v}\right) + 2\tan^{-1}\left(\frac{F^{-}\left(\frac{1}{2}+r\right)-u}{v}\right) - 2\alpha \\ &= 2\tan^{-1}\left(\frac{u-F^{-}\left(\frac{1}{2}+r\right)}{v}\right) + 2\tan^{-1}\left(\frac{F^{-}\left(\frac{1}{2}+r\right)-u}{v}\right) - 2\alpha \\ &= -2\alpha. \end{aligned}$$

Hence Θ has a symmetrical distribution around $-\alpha$. □

Corollary 7. *Since the distribution of* Θ *is symmetrical about* $-\alpha$

$$\begin{aligned} \mu &= \operatorname{atan}\left(E(\sin\Theta), E(\cos\Theta)\right) \\ &= -\alpha, \end{aligned}$$

$(E(\sin\Theta), E(\cos\Theta) < \infty)$ *where* $\operatorname{atan}(.,.)$ *is quadrant inverse tangent function defined as*

$$\operatorname{atan}(s,c) = \begin{cases} \tan^{-1}(s/c) & ,c > 0, s \geq 0 \\ \pi/2 & ,c = 0, s > 0 \\ \tan^{-1}(s/c) + \pi & ,c < 0 \\ \tan^{-1}(s/c) + 2\pi & ,c \geq 0, s < 0 \\ \textit{undefined} & ,c = 0, s = 0 \end{cases}.$$

In the following section, we show an application of the T_{α}^{-1} transformation to hyperbolic secant distribution. We introduce the methods for estimating the location parameter induced by T_{α}^{-1} in the relevant subsections. Also, that section includes the basic properties of the obtained circular distribution and an application to a real-life data set.

2. Induce Inverse Stereographic Hyperbolic Secant Model with Rotated Bilinear Transformations

Suppose X follows hyperbolic secant distribution, then cdf and pdf of X are

$$F(x) = \frac{2}{\pi}\tan^{-1}\left(e^{\frac{\pi}{2}x}\right), \tag{11}$$

$$f(x) = \frac{1}{2}\operatorname{sech}\left(\frac{\pi}{2}x\right), \quad x \in \mathbb{R} \tag{12}$$

respectively. This distribution is also called the inverse-cosh distribution because of the hyperbolic secant function is equivalent to the reciprocal hyperbolic cosine function. Note that the pdf given by Eq.(12) is symmetrical around $E(X) = 0$. By considering the Eq.(8) and Eq.(9) with Eq.(12) and Eq.(11), we obtain the cdf and pdf of the inverse stereographic hyperbolic secant distributed random variable $\Theta = T_\alpha^{-1}(X)$ as

$$G(\theta;\alpha,v) = \frac{2}{\pi}\tan^{-1}\left(e^{\frac{1}{2}\pi v\tan\left(\frac{\alpha+\theta}{2}\right)}\right), \tag{13}$$

$$g(\theta;\alpha,v) = \frac{v}{2(1+\cos(\alpha+\theta))}\operatorname{sech}\left[\frac{\pi v}{2}\tan\left(\frac{\alpha+\theta}{2}\right)\right], \tag{14}$$

respectively, where $v > 0$ is the scale parameter and $\alpha \in [-\pi,\pi)$ is the location parameter. In the rest of this paper, a random variable Θ having cdf as in Eq.(13) and pdf as in Eq.(14) will be denoted as $\Theta \sim ISHS(\alpha,v)$. Figure 2 illustrates the some of possible shapes of the pdf ofrandom variable $\Theta \sim ISHS(\alpha,v)$ for different values of the parameters α and v.

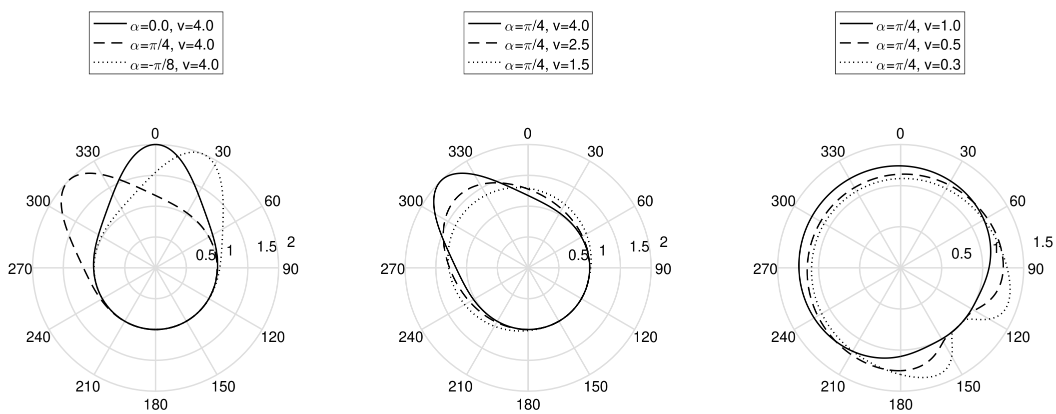

FIGURE 2. Pdf of $ISHS(\alpha,v)$ for different values of α and v.

Figure 2 shows that increasing α values cause counterclockwise rotation, and increasing v value causes an increase in angular concentration. The modality behavior of the ISHS distribution depends only the v parameter. For $v < 0.900316$, the distribution is bimodal. The modality behavior is studied more detailed in Subsection 2.3.

The inverse cdf of hyperbolic secant distribution is $F^{-1}(t) = -\frac{1}{\pi}\log\left(\cot^2\left(\frac{1}{2}\pi t\right)\right)$. Thus, the quantile function of $ISHS(\alpha,v)$ can be easily obtained from Eq.(10) as

$$Q(t) = -\alpha - 2\tan^{-1}\left[\frac{1}{\pi v}\log\left(\cot^2\left(\frac{\pi t}{2}\right)\right)\right], \tag{15}$$

where $t \in (0,1)$.

2.1. **Location, Dispersion and Median.** For a circular random variable, the pth cosine moment is defined as $c_p = E(\cos p\Theta)$, and the pth sine moment is defined as $s_p = E(\sin p\Theta)$ [7]. Thus, the mean direction is calculated as $\mu = \operatorname{atan}(s_1, c_1)$, where $\operatorname{atan}(.,.)$ is quadrant inverse tangent function. The explicit analytical forms of c_p and s_p values can not be obtained for random variable $\Theta \sim ISHS(\alpha, v)$. However, according to proposition 6 and corollary 7, it is clear that

$$\mu = \operatorname{atan}(s_1, c_1) = -\alpha.$$

The first trigonometric moments of Inverse Stereographic Hyperbolic Secant distribution are calculated numerically and presented in Figure 3. The following propositions give useful results for the location parameter of the $ISHS$ distribution.

Proposition 8. $\Theta \sim ISHS(\alpha, v) \Leftrightarrow -\Theta \sim ISHS(-\alpha, v)$.

Proposition 9. $\Theta \sim ISHS(\alpha, v) \Leftrightarrow \Theta + k \sim ISHS(\alpha - k, v)$

The length of mean direction vector is a measure of angular concentration around the mean and it is calculated as $\rho = \sqrt{c_1^2 + s_1^2}$. By using the value of ρ, the circular variance is calculated as $V = 1 - \rho$ and the circular standard deviation calculated as $\sigma = \sqrt{-2 \ln \rho}$. These three characteristics are illustrated in Figure 4 for different values of v.

As a measure of asymmetry, the skewness coefficient for the circular distribution is calculated as $\gamma_1 = \bar{s}_2 V^{-3/2}$, where $\bar{s}_p$ denotes the pth central sine moment which is defined as $\bar{s}_p = E[\sin p(\Theta - \mu)]$. According to the following proposition, the skewness coefficient of the $ISHS(\alpha, v)$ distribution are zero for every $v > 0$.

Proposition 10. *All central sine moments of $ISHS(\alpha, v)$ distribution is zero.*

Proof. Since $g(\theta; \alpha, v)$ is periodic with period 2π and $\mu = -\alpha$, we have

$$\begin{aligned} \bar{s}_p = E[\sin p(\Theta - \mu)] &= \int_{\theta_0}^{\theta_0 + 2\pi} \sin[p(\theta - \mu)]\, g(\theta; \alpha, v)\, d\theta \\ &= \int_{-\pi-\alpha}^{\pi-\alpha} \sin[p(\theta + \alpha)]\, g(\theta; \alpha, v)\, d\theta. \end{aligned}$$

According to proposition 9 $g(\theta; \alpha, v) = g(\theta + \alpha; 0, v)$, and according to proposition 6 $g(\theta; 0, v)$ is an even function. Thus, we can write $\bar{s}_p$ as

$$\bar{s}_p = \int_{-\pi}^{\pi} \sin(p\theta)\, g(\theta; 0, v)\, d\theta = 0$$

since $\sin(p\theta)\, g(\theta; 0, v)$ is an odd function. □

The kurtosis coefficient of a circular distribution is calculated as $\gamma_2 = \left(\bar{c}_2 - \rho^4\right)(1 - \rho)^{-2}$, where $\bar{c}_p$ denotes the pth central cosine moment and defined as $\bar{c}_p = E[\cos p(\Theta - \mu)]$. The change of the γ_2 value according to the parameter v of $ISHS(\alpha, v)$ distribution is shown in Figure 4.

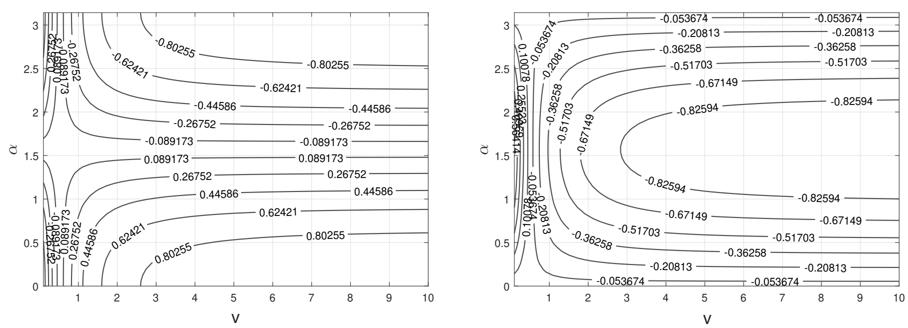

FIGURE 3. Contour plots for first cosine moment (left panel) and first sine moment (right panel) according to α and v.

The median direction (M) and the interquartile range (Iqr) of $ISHS(\alpha, v)$ distribution are easily obtained from Eq.(15), as follows, respectively:

$$M = Q\left(\frac{1}{2}\right) = -\alpha, \tag{16}$$

$$\begin{aligned} Iqr_\Theta &= Q(.75) - Q(.25) \\ &= 2\left(\tan^{-1}\left[\frac{2\log\left(\cot\left(\frac{\pi}{8}\right)\right)}{\pi v}\right] - \tan^{-1}\left[\frac{2\log\left(\tan\left(\frac{\pi}{8}\right)\right)}{\pi v}\right]\right) \\ &\simeq 4.\tan^{-1}\left(\frac{0.5611}{v}\right). \end{aligned}$$

2.2. **Entropy.** The entropy is a measure of variation or uncertainty of a random variable. Following the formal definition of the entropy, the entropy of the random variable $\Theta \sim ISHS(\alpha, v)$ is

$$H_\Theta = -\int_\Gamma g(\theta; \alpha, v) \ln g(\theta; \alpha, v)\, d\theta,$$

where Γ is any interval of length 2π. Since Θ is 2π periodic

$$\begin{aligned} H_\Theta &= -\int_\Gamma g(\theta; 0, v) \ln g(\theta; 0, v)\, d\theta \\ &= -v\int_\Gamma \frac{\operatorname{sech}\left(\frac{1}{2}\pi v \tan\left(\frac{\theta}{2}\right)\right)}{2\cos(\theta) + 2} \log\left(v\frac{\operatorname{sech}\left(\frac{1}{2}\pi v \tan\left(\frac{\theta}{2}\right)\right)}{2\cos(\theta) + 2}\right) d\theta. \end{aligned} \tag{17}$$

We could not get an explicit analytical form of the integral in Eq.(17). Therefore, we numerically calculated the H_Θ with respect to v and illustrated in Figure 4. Note that the entropy of the circular uniform distribution is $\ln(2\pi)$ and this is the maximum entropy any circular distribution may have. Figure 4 shows that the maximum value of the H_Θ is below this value. The entropy of the $ISHS$ distribution attains its maximum value when the circular variance is maximized or equivalently angular concentration minimized. Thus one can write

$$\begin{aligned} v^* &= \text{argmax}_{\,v>0} H_\Theta = \text{argmin}_{v>0}\, c_1 \\ &= \text{argmin}_{v>0} \int_\Gamma \cos(\theta)\, g(\theta; 0, v)\, d\theta \\ &= \text{argmin}_{v>0} \int_0^\pi \cos(\theta)\, g(\theta; 0, v)\, d\theta. \end{aligned}$$

Since the minimum value of the first cosine moment is zero, the value of v^* is obtained by solving the equation

$$\int_0^\pi \cos(\theta)\, g(\theta; 0, v)\, d\theta = 0$$

with respect to v. Using the bisection method, we observed that $v^* \simeq 0.521567$.

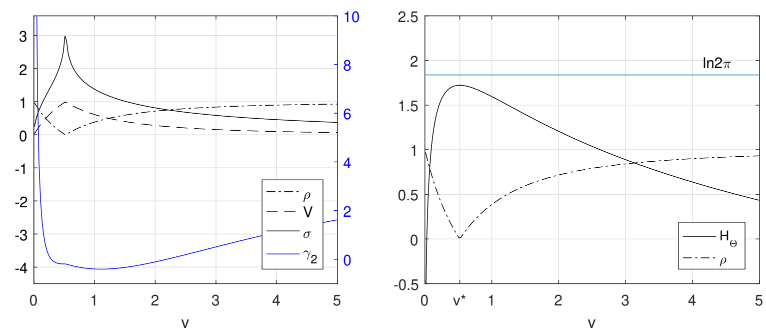

FIGURE 4. Values of ρ,V,σ (left axis) and γ_2 (right axis) according to v (left panel). Entropy and ρ values according to v (right panel).

2.3. **Modality.** The ISHS distribution is unimodal or bimodal depending on the value of the v parameter. Therefore, it will be sufficient to examine the modality behavior of the $g(\theta; 0, v)$ function, which is symmetric about 0 when $\Gamma = [-\pi, \pi)$. The first and second derivates of $g(\theta; 0, v)$ with respect to θ are

$$g'(\theta; 0, v) = -\frac{v\, \text{sech}\left(\frac{1}{2}\pi v \tan\left(\frac{\theta}{2}\right)\right)\left(\pi v \tanh\left(\frac{1}{2}\pi v \tan\left(\frac{\theta}{2}\right)\right) - 2\sin(\theta)\right)}{4(\cos(\theta) + 1)^2}$$

and

$$g''(\theta;0,v)=\frac{v\operatorname{sech}\left(\frac{1}{2}\pi v\tan\left(\frac{\theta}{2}\right)\right)}{8(\cos(\theta)+1)^3}$$
$$\times\left[4\cos(\theta)-2\cos(2\theta)+6+\pi v\left(\begin{array}{c}-2\pi v\operatorname{sech}^2\left(\frac{1}{2}\pi v\tan\left(\frac{\theta}{2}\right)\right)\\ -6\sin(\theta)\tanh\left(\frac{1}{2}\pi v\tan\left(\frac{\theta}{2}\right)\right)\\ +\pi v\end{array}\right)\right]$$

respectively. Since $g(\theta;0,v)$ is symmetric around 0, $\theta=0$ is a saddle point, ie $g'(0;0,v)=0$. If this point is a local minimum, then $g''(0;0,v)>0$. Thus, ISHS distribution is bimodal when $g''(0;0,v)=-64^{-1}v\left(\pi^2v^2-8\right)>0\iff v<2\sqrt{2}/\pi\simeq 0.900316$.

2.4. **Order Statistics.** Let $\Theta_1,\Theta_2,...,\Theta_n$ be a random sample from $ISHS(\alpha,v)$ distribution and let $\Theta_{(1)}\leq\Theta_{(2)}\leq\ldots\leq\Theta_{(n)}$ denote the order statistic for this sample. Then, the pdf of the random variable $\Theta_{(i)}$, $i=1,2,...,n$ is obtained as

$$\begin{aligned}h_{\Theta_{(i)}}(\theta;\alpha,v)&=\frac{n!}{(i-1)!(n-i)!}G(\theta;\alpha,v)^{i-1}g(\theta;\alpha,v)(1-G(\theta;\alpha,v))^{n-i}\\&=\frac{2^{i-2}\pi^{1-i}vn!\tan^{-1}\left(e^{\frac{1}{2}\pi v\tan\left(\frac{\alpha+\theta}{2}\right)}\right)^{i-1}}{(i-1)!(n-i)!(\cos(\alpha+\theta)+1)}\\&\quad\times\operatorname{sech}\left(\frac{1}{2}\pi v\tan\left(\frac{\alpha+\theta}{2}\right)\right)\left(1-\frac{2\tan^{-1}\left(e^{\frac{1}{2}\pi v\tan\left(\frac{\alpha+\theta}{2}\right)}\right)}{\pi}\right)^{n-i}.\end{aligned}\tag{18}$$

The pdf of first order (minimum) and nth order (maximum) statistics can be immediately calculated from Eq.(18) as

$$h_{\Theta_{(1)}}(\theta;\alpha,v)=\frac{\operatorname{sech}\left(\frac{1}{2}\pi v\tan\left(\frac{\alpha+\theta}{2}\right)\right)}{2\cos(\alpha+\theta)+2}nv\left(1-\frac{2\tan^{-1}\left(e^{\frac{1}{2}\pi v\tan\left(\frac{\alpha+\theta}{2}\right)}\right)}{\pi}\right)^{n-1}$$

and

$$h_{\Theta_{(n)}}(\theta;\alpha,v)=\frac{\operatorname{sech}\left(\frac{1}{2}\pi v\tan\left(\frac{\alpha+\theta}{2}\right)\right)}{(\cos(\alpha+\theta)+1)}2^{n-2}\pi^{1-n}nv\tan^{-1}\left(e^{\frac{1}{2}\pi v\tan\left(\frac{\alpha+\theta}{2}\right)}\right)^{n-1},$$

respectively.

2.5. **Inference.** In this section, we consider estimating the unknown parameters of $ISHS(\alpha,v)$ distribution. We will use tree methods commonly used in the literature, such as, maximum likelihood (ml), weighted least-squares (ls) and moments estimation (me) methods. Finally, a Monte-Carlo simulation study will be given to show and compare the performance of ml, me and ls estimators.

2.5.1. *Maximum Likelihood Estimation.* Let $\Theta_1, \Theta_2, ..., \Theta_n$ be a random sample from $ISHS\left(\alpha, v\right)$ distribution. By considering the random variables $\Theta_i, i = 1, 2, ..., n$, The logarithmic likelihood function of α and v can be written as

$$L\left(\alpha, v; \theta_1, \theta_2, ..., \theta_n\right) = \sum_{i=1}^{n} \log\left[\frac{1}{4} v \sec^2\left(\frac{\alpha+\theta_i}{2}\right) \operatorname{sech}\left(\frac{1}{2}\pi v \tan\left(\frac{\alpha+\theta_i}{2}\right)\right)\right].$$

If the first derivatives of this log-likelihood function with respect to parameters α and v are taken and equalized them to zero, then we have the following normal equations

$$\frac{\partial L}{\partial \alpha} = \sum_{i=1}^{n} \tan\left(\frac{1}{2}\left(\alpha+\theta_i\right)\right) - \frac{1}{4}\pi v \sum_{i=1}^{n} \sec^2\left(\frac{\alpha+\theta_i}{2}\right) \tanh\left(\frac{1}{2}\pi v \tan\left(\frac{\alpha+\theta_i}{2}\right)\right) = 0 \tag{19}$$

and

$$\frac{\partial L}{\partial v} = \frac{n}{v} - \frac{\pi}{2} \sum_{i=1}^{n} \tan\left(\frac{\alpha+\theta_i}{2}\right) \tanh\left(\frac{1}{2}\pi v \tan\left(\frac{\alpha+\theta_i}{2}\right)\right) = 0. \tag{20}$$

Let us denote the ml estimates of the parameters α and v as $\widehat{\alpha}_{ML}$ and $\widehat{v}_{ML}$, respectively. Hence, $\widehat{\alpha}_{ML}$ and $\widehat{v}_{ML}$ can obtained from the collective solution of Eq.(19) and Eq.(20). However, these equations do not have an analytical solution. So $\widehat{\alpha}_{ML}$ and $\widehat{v}_{ML}$ must be obtained numerically.

2.5.2. *Weighted Least Square Estimation.* A well-known modification of least square estimation method is the weighted least square, which has a lower bias than the ordinary least square estimation. Let us consider the ordered random sample $\theta_{(1)} < \cdots < \theta_{(n)}$ from $ISHS\left(\alpha, v\right)$ distribution. The weighted least square estimates of the parameters, say $\widehat{\alpha}_{LS}$ and $\widehat{v}_{LS}$ are obtained by minimizing

$$\sum_{j=1}^{n} \frac{\left(n+1\right)^2\left(n+2\right)}{j\left(n-j+1\right)} \left[\frac{2}{\pi} \tan^{-1}\left(e^{\frac{1}{2}\pi v \tan\left(\frac{\alpha+\theta_{(j)}}{2}\right)}\right) - \frac{j}{n+1}\right]^2, \tag{21}$$

with respect to α and v. Where $\frac{j}{n+1}$ is the expectation of the empirical distribution function of the ordered data, see Swain et al. [10]. Numerical methods can be used to minimize Eq.(21).

2.5.3. *Method of Moment Estimation.* Let us start by expressing the sample trigonometric moments for circular data [7]. The pth order sample cosine moment is defined as

$$\overline{C}_p = \frac{1}{n} \sum_{i=1}^{n} \cos\left(p\theta_i\right),$$

and sample sine moment is defined as

$$\overline{S}_p = \frac{1}{n} \sum_{i=1}^{n} \sin\left(p\theta_i\right).$$

Now consider the random sample $\theta_1, \theta_2, \ldots, \theta_n$ from the $ISHS(\alpha, v)$ distribution. Moment estimates of α and v ($\widehat{\alpha}_{ME}$ and $\widehat{v}_{ME}$) are obtained from the collective solution of equations

$$\overline{C}_1 - c_1 = 0, \tag{22}$$

and

$$\overline{S}_1 - s_1 = 0 \tag{23}$$

by using numerical methods, where $c_1 = E(\cos\Theta)$ and $s_1 = E(\sin\Theta)$.

2.5.4. *Monte-Carlo Simulation Study.* We perform some Monte-Carlo experiments to compare the performance of ml, ls, and me estimators in different sample sizes. We consider $n = 50, 100, 500,$ and 1000 sample sizes and the repitation of the simulation is set as 100 times in each sample size. The algorithm below has been run for different parameter sets and the results are shown in Table 1.

Step 1. Select n and set values of the parameters α and v.
Step 2. Generate n random numbers from $U(0,1) \to u_{n\times1}$.
Step 3. Calculate $Q(u_{n\times1}) \to \theta_{n\times1}$, where $Q(.)$ as Eq.(15).
Step 4. Get $\widehat{\alpha}_{ML}$ and $\widehat{v}_{ML}$ from the collective solution of Eq.(19) and Eq.(20).
Get $\widehat{\alpha}_{LS}$ and $\widehat{v}_{LS}$ from minimazing Eq.(21).
Get $\widehat{\alpha}_{ME}$ and $\widehat{v}_{ME}$ from the collective solution of Eq.(22).and Eq.(23).
Step 5. Repeat Step 2 to Step 4 for $N = 100$ times.
Step 6. Calculate the $|Bias(.)|$ and $Mse(.)$ values of the $\widehat{\alpha}$ and $\widehat{v}$ estimators for each ml, ls, and me estimates.

As we discussed in relevant sections, the referred equations in Step 4 have no analytical solutions. We carried out the programming in Matlab and used the 'fsolve' subroutine to solve Eq.(19), Eq.(20), Eq.(22), and Eq.(23). For the minimization problem in Eq.(21), we used the 'fmincon' subroutine. In all routines, the initial values of parameters were taken as $-m_1 = -\operatorname{atan}\left(\overline{S}_1, \overline{C}_1\right)$ for α and 1 for v.

According to the results in Table 1, it is seen that the Bias and MSE values decrease to zero as the sample size increases for the estimation of parameters α and v by all three methods. This shows that the estimates are precise and accurate, hence, we say that it is consistent and unbiased. It is known that ml estimators are asymptotically unbiased estimators. So, the results in Table 1 agree with expectations for ml estimators. In addition, simulation results show that the other estimators have the same characteristics.

Table 1. Simulated Bias and MSE values of parameter estimates for different sample sizes and parameter values.

			$\alpha = \pi/2$				$\alpha = -\pi/4$			
			$\widehat{\alpha}$		$\widehat{v}$		$\widehat{\alpha}$		$\widehat{v}$	
	Method	n	Bias	MSE	Bias	MSE	Bias	MSE	Bias	MSE
v=3	ML	50	.0067	.0058	.0551	.1663	.0021	.0068	.0950	.2064
		100	.0051	.0031	.1007	.0840	.0098	.0033	.0533	.0954
		500	.0017	.0007	.0057	.0160	.0019	.0006	.0204	.0163
		1000	.0017	.0003	.0040	.0068	.0018	.0003	.0104	.0067
	ME	50	.0066	.0058	.0619	.1703	.0026	.0070	.1012	.2169
		100	.0057	.0031	.1007	.0831	.0075	.0032	.0605	.1005
		500	.0023	.0007	.0031	.0171	.0018	.0006	.0198	.0168
		1000	.0016	.0003	.0038	.0070	.0016	.0003	.0070	.0070
	LS	50	.0070	.0057	.0226	.1883	.0018	.0071	.0088	.2178
		100	.0052	.0030	.0745	.0910	.0081	.0032	.0177	.1029
		500	.0020	.0007	.0082	.0178	.0021	.0006	.0171	.0171
		1000	.0015	.0003	.0062	.0072	.0019	.0003	.0099	.0071
v=6	ML	50	.0049	.0015	.1384	.6167	.0064	.0014	.0302	.4931
		100	.0024	.0010	.0401	.2787	.0005	.0010	.0963	.3519
		500	.0021	.0001	.0189	.0554	.0024	.0002	.0165	.0556
		1000	.0003	.0001	.0072	.0264	.0002	.0001	.0085	.0284
	ME	50	.0049	.0017	.2071	.5840	.0047	.0017	.0538	.5626
		100	.0031	.0010	.0710	.2968	.0001	.0011	.1093	.4181
		500	.0020	.0001	.0502	.0677	.0024	.0002	.0132	.0626
		1000	.0005	.0001	.0270	.0305	.0007	.0001	.0029	.0321
	LS	50	.0049	.0016	.0183	.8181	.0062	.0015	.0939	.5589
		100	.0026	.0010	.0021	.3388	.0005	.0010	.0534	.3494
		500	.0022	.0001	.0037	.0595	.0024	.0002	.0130	.0605
		1000	.0003	.0001	.0049	.0292	.0003	.0001	.0159	.0292
v=0.75	ML	50	.0062	.0114	.0342	.0115	.0117	.0125	.0298	.0122
		100	.0105	.0068	.0126	.0043	.0008	.0056	.0086	.0042
		500	.0046	.0011	.0023	.0008	.0015	.0011	.0018	.0010
		1000	.0008	.0005	.0005	.0004	.0028	.0005	.0014	.0005
	ME	50	.0776	.4152	.0358	.0235	.0130	.4464	.0203	.0266
		100	.0825	.2560	.0102	.0092	.0658	.2579	.0059	.0097
		500	.0111	.0254	.0044	.0010	.0170	.0256	.0003	.0012
		1000	.0235	.0108	.0016	.0005	.0111	.0105	.0023	.0005
	LS	50	.0232	.0412	.0324	.0159	.0107	.0309	.0202	.0140
		100	.0219	.0147	.0074	.0049	.0058	.0139	.0045	.0050
		500	.0003	.0026	.0019	.0008	.0023	.0028	.0021	.0011
		1000	.0003	.0014	.0001	.0004	.0001	.0013	.0015	.0005

2.6. **Real Data Example.** In this section, we study the modeling behavior of the ISHS distribution on a real-life dataset. We consider the termite mounds data in Appendix B.13 (set 7) of Fisher [3]. The data consist of $n = 66$ termite mounds orientations of Amitermes laurensis in the Cape York Peninsula, North Queensland. We obtained the parameter estimates by using Matlab's 'fmincon' and 'fsolve' subroutines. In these subroutines, the parameter ranges were chosen as wide as possible to avoid local maxima. The initial values were set to $-m_1 = -\operatorname{atan}\left(\overline{S}_1, \overline{C}_1\right)$ for α and 1 for v. In order to make comparisons, we chosed the Von-Mises (VM) and Wrapped Cauchy (WC) distributions as well-known alternatives from the location family for modeling symmetrical circular data. Table 2 shows the parameter estimates for each models, and Figure 5 illustrates the fitted pdfs and cdfs. The ISHS parameters were estimated with three methods; ml, me and ls. Table 2 also includes the mean direction and resultant length estimates for each models, and the values of these characteristics obtained from the sample.

Table 2. Parameter estimates, estimated mean direction and resultant length for termit mounds data.

Model	Method	Parameters		Mean Direction	Res. Length	Iqr
		$\widehat{\alpha}$	$\widehat{v}$			
ISHS	ML	-3.0527	6.7146	3.0527 (174.91°)	0.9596	0.3335
	ME	-3.0381	6.4753	3.0381 (174.07°)	0.9569	0.3457
	LS	-3.0551	6.9872	3.0551 (175.04°)	0.9625	0.3205
		$\widehat{\mu}$	$\widehat{\kappa}$			
VM	ML	3.0381	11.8567	3.0381 (174.07°)	0.9569	0.3968
		$\widehat{\mu}$	$\widehat{\gamma}$			
WC	ML	3.0485	0.14748	3.0485 (174.66°)	0.8566	0.2974
Sample	-	-	-	3.0381 (174.07°)	0.9569	0.3491

Table 3 contains Log-likelihood (LL), the Akaike and Bayesian information criteria (AIC and BIC), Watson's $U^2(W^2)$ statistics values, Kolmogorov-Smirnov (KS) and Chi square tests statistics with p-values. Here, it is seen that the data fit all the distributions selected ($p > 0.05$). However, it can be said that the proposed ISHS model is the model that best fits the data since it has the smallest values in all model selection criteria.

TABLE 3. Summary of fits for termit mounds data.

Model		-LL	AIC	BIC	W^2	K-S (p)	Chi sq.(p)
ISHS	ML	10.559	25.118	29.497	.040	.06 (.9478)	3.24 (.3557)
	ME	10.710	25.419	29.799	.038	.06 (.9487)	3.70 (.2953)
	LS	10.628	25.255	29.634	.054	.09 (.6460)	3.05 (.3836)
VM	ML	13.537	31.073	35.453	.104	.11 (.3393)	6.21 (.1017)
WC	ML	16.768	37.537	41.916	.085	.10 (.4779)	5.52 (.1372)

Plots of the fitted densities are shown in Figure 5. Left panel of this figure represents the circular data plot, fitted pdfs of the ISHS distribution with ml, me and ls estimates, fitted vm and wc models. The arrow points out the sample mean resultant vector

$$m_1 = \operatorname{atan}\left(\overline{S}_1, \overline{C}_1\right)$$
$$= 3.0381\,(174.07^\circ)\,,$$

and resultant length

$$r_1 = \sqrt{\overline{C}_1^2 + \overline{S}_1^2}$$
$$= 0.4971,$$

where $\overline{C}_1$ and $\overline{S}_1$ the first order sample cosine and sine moments, respectively.

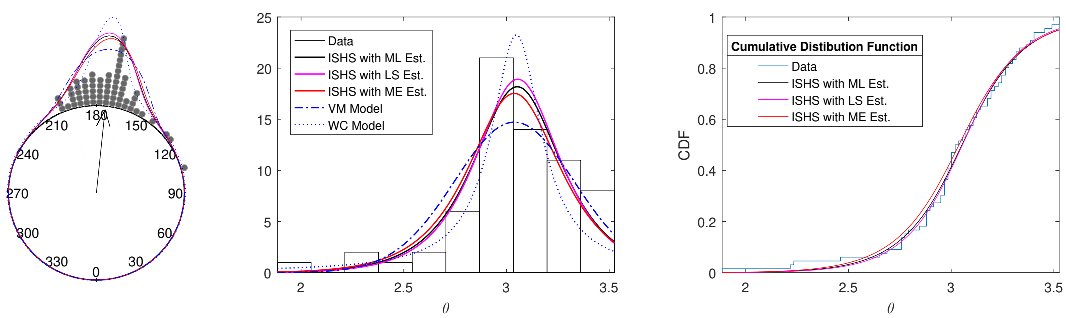

FIGURE 5. Plots for termite mounds data. Circular data plot, fitted circular pdfs (left) linear histogram and fitted pdfs (center), empirical cdf and fitted cdfs (rigth).

All models estimated the average orientation of the mounds to be almost south. The ISHS model with ME estimates gave the mean orientation and resultant length the same as in the sample. This is an expected result for moment estimators. Same thing valid for the VM model. However, when we compare the modeling performances with the values in Table 3, we see that the ISHS model is better than both the VM and the WC model.

3. Conclusion

After Minh and Farnum [8] introduced the ISP method, a number of researchers have introduced many circular distributions by employing the ISP method. In some of these (for example; [1], [4] and [6]), the authors added a location parameter to the circular distributions in their studies. In fact, the location parameter to be added to the circular probability distributions obtained by the ISP method corresponds to the rotation property of bilinear transforms. Here, the rotation means fixing the origin and rotating all other points by the same amount and counterclockwise. In this study, we considered rotation in bilinear transformations and used the rotated inverse stereographic projection (T_α^{-1}) to obtain a new circular model. Thus, we showed that the circular model to be obtained by the $T_\alpha^{-1}(X)$ transformation will naturally belong to the location family of the distributions. Before the section including the application of the method, we gave some propositions and theorems that are useful when the transformation is applied to especially symmetric distributions. In the study, we applied T_α^{-1} to the hyperbolic secant distribution. Thus, we obtained a symmetrical circular distribution with two parameters. One of these parameters is the location parameter and induced by rotated inverse stereographic projection T_α^{-1}. To estimate the unknown parameters of the introduced distribution, the maximum likelihood, the weighted least squares, and the moment estimators are obtained. By a conducted Monte Carlo simulation study, we show that, as the sample size increases, both Bias and MSE values decrease for all estimation methods. Finally, we used the introduced distribution on a real dataset. To compare the fitting performance, we considered the Von-Mises distribution (also known as the circular normal distribution) and Wrapped Cauchy distribution as well-known symmetric alternatives. We observed that the fitting performance of the obtained distribution according to the measures frequently used in the literature is better than both Von-Mises and Wrapped Cauchy distribution.

Declaration of Competing Interests The author declares that he has no known competing financial interests or personal relationships that could affect the work reported in this article.

References

[1] Chaubey, Y. P., Karmaker, S. C., On some circular distributions induced by inverse stereographic projection, *Sankhya B* (2019), 1–23, https://dx.doi.org/https://doi.org/10.1007/s13571-019-00201-1.

[2] Dattatreya Rao, A., Girija, S., Phani, Y., Stereographic logistic model-application to noisy scrub birds data, *Chilean Journal of Statistics,* 7 (2) (2016), 69–79.

[3] Fisher, N. I., Lewis, T., Embleton, B. J., Statistical Analysis of Spherical Data, Cambridge University Press, 1993.

[4] Girija, S., Rao, A., Yedlapalli, P., On stereographic lognormal distribution, *International Journal of Advances in Applied Sciences, 2* (3) (2013), 125–132.

[5] Girija, S., Rao, A. D., Yedlapalli, P., New circular model induced by inverse stereographic projection on double exponential model-application to birds migration data, *Journal of Applied Mathematics, Statistics and Informatics, 10* (1) (2014), 5–17, https://dx.doi.org/https://doi.org/10.2478/jamsi-2014-0001.

[6] Kato, S., Jones, M., A family of distributions on the circle with links to, and applications arising from, möbius transformation, *Journal of the American Statistical Association, 105* (489) (2010), 249–262, https://dx.doi.org/https://doi.org/10.1198/jasa.2009.tm08313.

[7] Mardia, K. V., Jupp, P. E., Directional Statistics, vol. 494, John Wiley & Sons, 2009.

[8] Minh, D. L., Farnum, N. R., Using bilinear transformations to induce probability distributions, *Communications in Statistics-Theory and Methods, 32* (1) (2003), 1–9, https://dx.doi.org/https://doi.org/10.1081/STA-120017796.

[9] Needham, T., Visual Complex Analysis, Oxford University Press, 1998.

[10] Swain, J. J., Venkatraman, S., Wilson, J. R., Least-squares estimation of distribution functions in johnson's translation system, *Journal of Statistical Computation and Simulation, 29* (4) (1988), 271–297, https://dx.doi.org/https://doi.org/10.1080/00949658808811068.

[11] Yedlapalli, P., Girija, S., Dattatreya Rao, A., Srihari, G., Symmetric circular model induced by inverse stereographic projection on double weibull distribution with application, *International Journal of Soft Computing, Mathematics and Control, 4* (2015), 69–76, https://dx.doi.org/https://doi.org/10.14810/ijscmc.2015.4106.

[12] Yedlapalli, P., Sastry, K., Rao, A., On stereographic semicircular quasi lindley distribution, *Journal of New Results in Science, 8* (2019), 6 – 13.